

SUPPORTING INFORMATION

Rational Design of BODIPY Functionalized MOF Photocatalysts for Highly Efficient Hydrogen Production

Zehra Coşkun^a, Elif Yıldız Gül^{a,b}, Burcu Topaloğlu Aksoy^a, Azam Seifi^c, Esra Tanrıverdi Eçik^b,

Bünyemin Çoşut^{*a}

^aDepartment of Chemistry, Gebze Technical University, 41400, Gebze, Türkiye

^bDepartment of Chemistry, Atatürk University, 25240, Erzurum, Türkiye

^cDepartment of Environmental Engineering, Kocaeli University, Türkiye

* Author for correspondence:

Dr. Bünyemin Çoşut, Department of Chemistry, Gebze Technical University, Gebze 41400,
Kocaeli, Turkey

Tel: 00 90 262 6053015

Fax: 00 90 262 6053105

e-mail: bcosut@gtu.edu.tr

TABLE OF CONTENTS

Fig. S1: Synthesis of BD1, BD2, BD3, BD4 and UiO-66-NH ₂	3
Synthesis of BD1	4
Synthesis of BD3	4
Synthesis of UiO-66-NH₂	5
Fig. S2: The ¹ H NMR spectrum of BD1	6
Fig. S3: The ¹³ C NMR spectrum of BD1	6
Fig. S4: The ¹ H NMR spectrum of BD3	7
Fig. S5: The ¹³ C NMR spectrum of BD3	7
Fig. S6: The MALDI TOF mass spectrum of BD2	8
Fig. S7: The ¹ H NMR spectrum of BD2	8
Fig. S8: The ¹³ C NMR spectrum of BD2	9
Fig. S9: The MALDI TOF mass spectrum of BD4	9
Fig. S10: The ¹ H NMR spectrum of BD4	10
Fig. S11: The ¹³ C NMR spectrum of BD4	10
Fig. S12: FT-IR spectrums of (A) BD2/UiO-66-NH ₂ , (B) BD4/UiO-66-NH ₂	11
Fig. S13: HRTEM images of UiO-66-NH ₂ (A) 10 nm, (B) 20 nm, (C) 200 nm, (D) 500 nm	12
Fig. S14: HRTEM images of BD4/UiO-66-NH ₂ (A) 10 nm, (B) 20 nm, (C) 100 nm	12
Fig. S15: Absorbance and reflectance spectrums of UiO-66-NH ₂	13
Fig. S16: Absorbance and reflectance spectrums of BD2/UiO-66-NH ₂	13
Fig. S17: Absorbance and reflectance spectrums of BD4/UiO-66-NH ₂	14
Fig. S18: FTIR spectrums of BD4/UiO-66-NH ₂ (A) before HER, (B) after HER	14
Fig. S19: PXRD pattern of BD4/UiO-66-NH ₂ (A) before HER, (B) after HER	15

Fig. S20: SEM images of BD4/UiO-66-NH₂ (A) before HER, (B) after HER

15

Fig. S21: H₂ Evolution Comparison of BD4 and BD4/UiO-66-NH₂

16

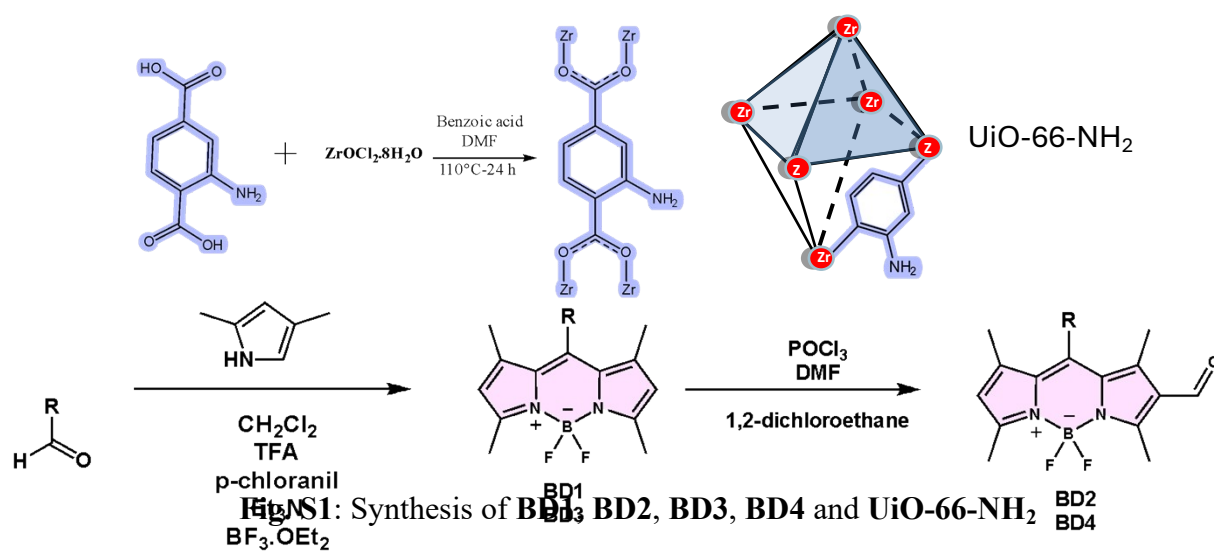
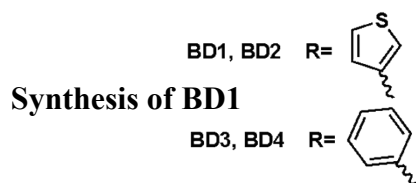


Fig. S1: Synthesis of **BD1**, **BD2**, **BD3**, **BD4** and **UiO-66-NH₂**



BD1 was synthesized according to the literature (38). 2,4-dimethylpyrrole (1 mL, 9.7 mmol) was added in the reaction flask after 200 mL of CH₂Cl₂ was purged with Ar for 30 min. Then, the reaction medium was purged with Ar for additional 10 min. 3-thiophenecarboxaldehyde (0.40 mL, 4.6 mmol) was added to the reaction medium. A few drops of trifluoroacetic acid was added later. The mixture was allowed to stir under Ar atm at room temperature for 3 hours. p-chloranil (1.13 g, 4.6 mmol) was added and the reaction mixture was stirred for 2 hours. 5 mL of Et₃N and 5 mL BF₃.OEt₂ was added to the reaction mixture dropwise, respectively. The reaction mixture was allowed to stir at room temperature for 3 hours and was extracted with water and organic layer was dried using Na₂SO₄. The crude product was purified by silica gel column chromatography using n-hexane:CH₂Cl₂ (3:1) as eluent to give **BD1** (orange solid, 200 mg, 13%) (Fig. S1). ¹H NMR (400 MHz, CDCl₃) δ_H (ppm): 7.41 (m, 1H, Ar-H), 7.11 (m, 1H, Ar-H), 6.89 (m, 1H, Ar-H), 5.91 (s, 2H, Ar-H), 2.47 (s, 6H, -CH₃), 1.42 (s, 6H, -CH₃) (Fig. S2). ¹³C NMR (101 MHz, CDCl₃) δ_C (ppm): 155.53, 143.14, 137.00, 134.50, 131.76, 127.48, 127.39, 123.78, 121.19, 14.61, 13.70 (Fig. S3).

Synthesis of **BD3**

BD3 was synthesized according to the literature (39). 2,4-dimethylpyrrole (1 mL, 9.7 mmol) was added in the reaction flask after 200 mL of CH₂Cl₂ was purged with Ar for 30 min. Then, the reaction medium was purged with Ar for an additional 10 min. Benzaldehyde (0.45 mL, 4.4 mmol) was added to the reaction medium. A few drops of trifluoroacetic acid were added later. The mixture was allowed to stir under Ar atm at room temperature for 3 hours. p-chloranil (1.08 g, 4.4 mmol) was added and the reaction mixture was stirred for 2 hours. 5 mL of Et₃N and 5 mL BF₃.OEt₂ was added to the reaction mixture dropwise respectively. The reaction mixture was allowed to stir at room temperature for 3 hours and was extracted with water and organic layer was dried using Na₂SO₄. The crude product was purified by silica gel column chromatography using n-

hexane:CH₂Cl₂ (3:1) as eluent to **BD3** (orange solid, 200 mg, 13%). ¹H NMR (400 MHz, CDCl₃) δ_H (ppm): 7.51 (m, 3H) (Ar-H), 7.30 (m, 2H) (Ar-H), 6.00 (s, 2H) (Ar-H), 2.58 (s, 6H) (-CH₃), 1.39 (s, 6H) (-CH₃) (Fig. S4). ¹³C NMR (101 MHz, CDCl₃) δ_C (ppm): 155.42, 143.17, 141.74, 134.99, 131.43, 129.14, 128.95, 127.93, 121.22, 14.60, 14.36 (Fig. S5).

Synthesis of UiO-66-NH₂

UiO-66-NH₂ was synthesized according to the literature with some modifications (40). Initially, 1.5 g (4.65 mmol) of ZrOCl₂·8H₂O, 1.0 g (5.52 mmol) of NH₂-BDC, and 25.0 g (204.7 mmol) of benzoic acid were placed into a 250 mL glass bottle. Subsequently, 100 mL of DMF was added, and the mixture was sonicated in an ultrasonic bath until the solid components had completely dissolved, yielding a homogeneous solution. The reaction mixture was then placed in an oven and kept at 110°C for 24 hours. Upon completion of the reaction, the product was collected by centrifugation and thoroughly washed with DMF and acetone to remove unreacted residues and by-products. Finally, the material was dried overnight in an oven at 60°C, followed by additional drying under vacuum at 100°C. The resulting product was then subjected to characterization analyses.

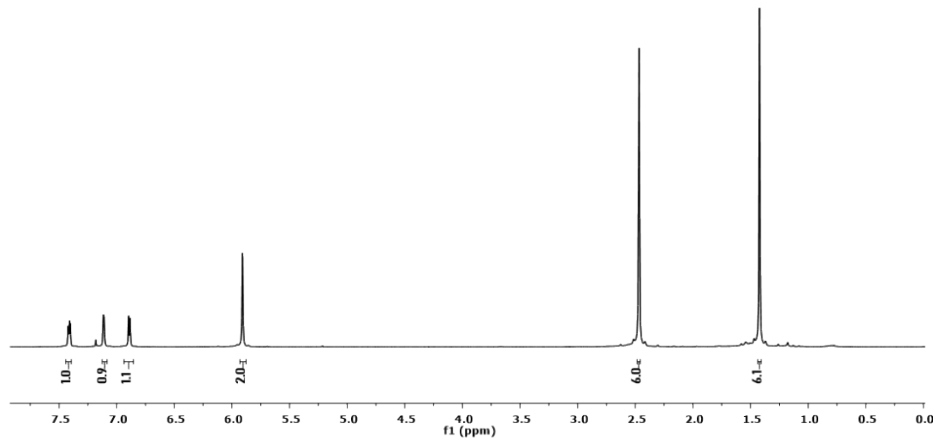


Fig. S2: The ¹H NMR spectrum of **BD1**

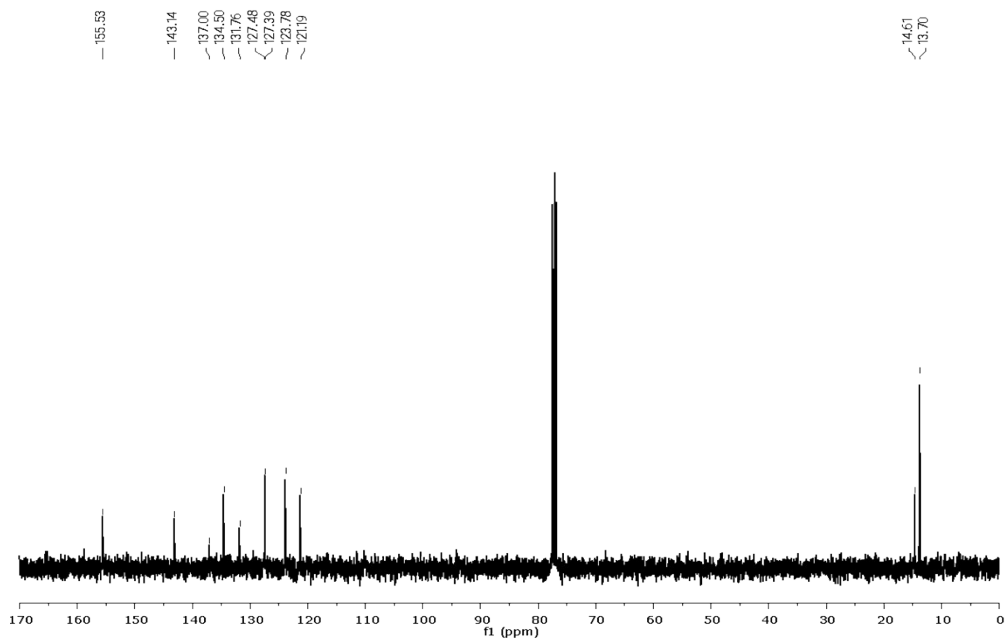


Fig. S3: The ¹³C NMR spectrum of **BD1**

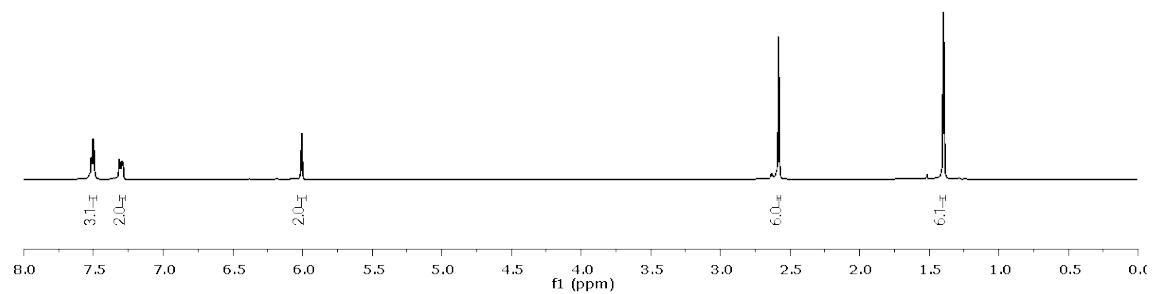


Fig. S4: The ^1H NMR spectrum of **BD3**

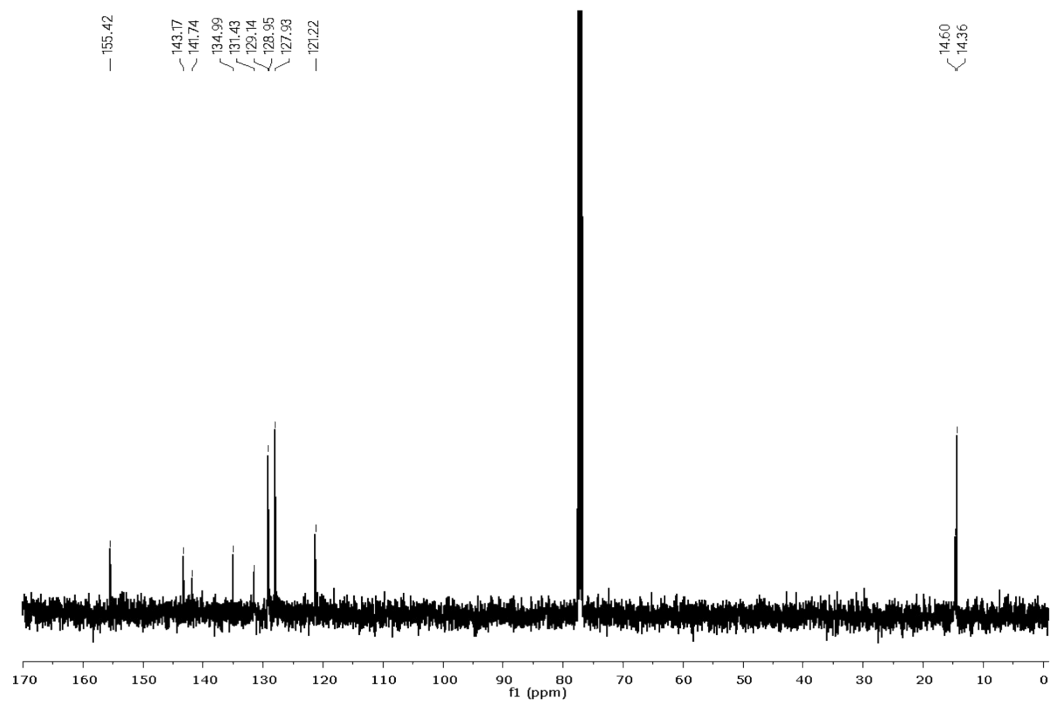


Fig. S5: The ^{13}C NMR spectrum of **BD3**

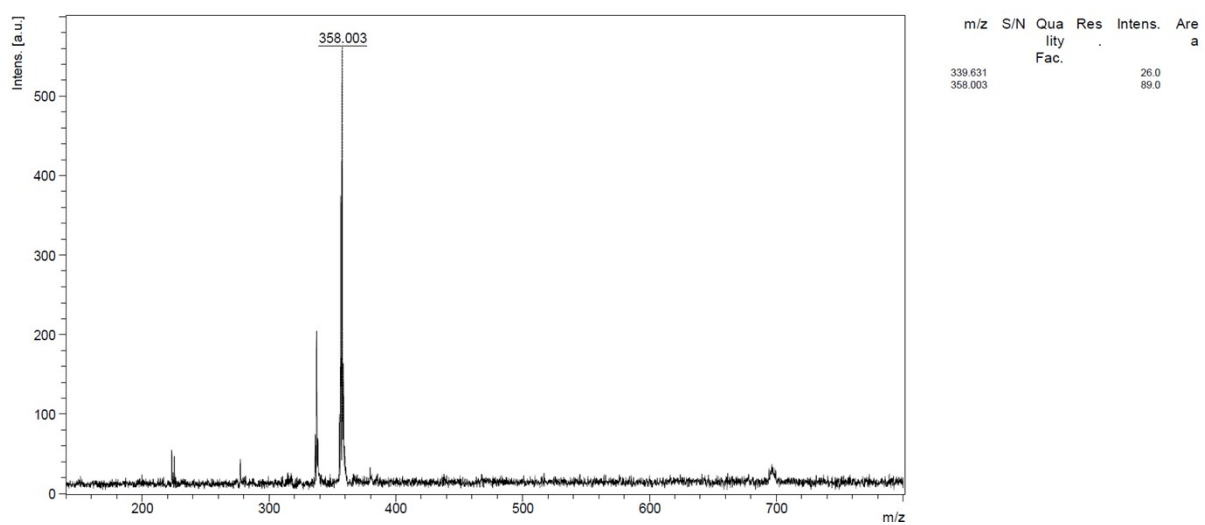


Fig. S6: The MALDI TOF mass spectrum of **BD2**

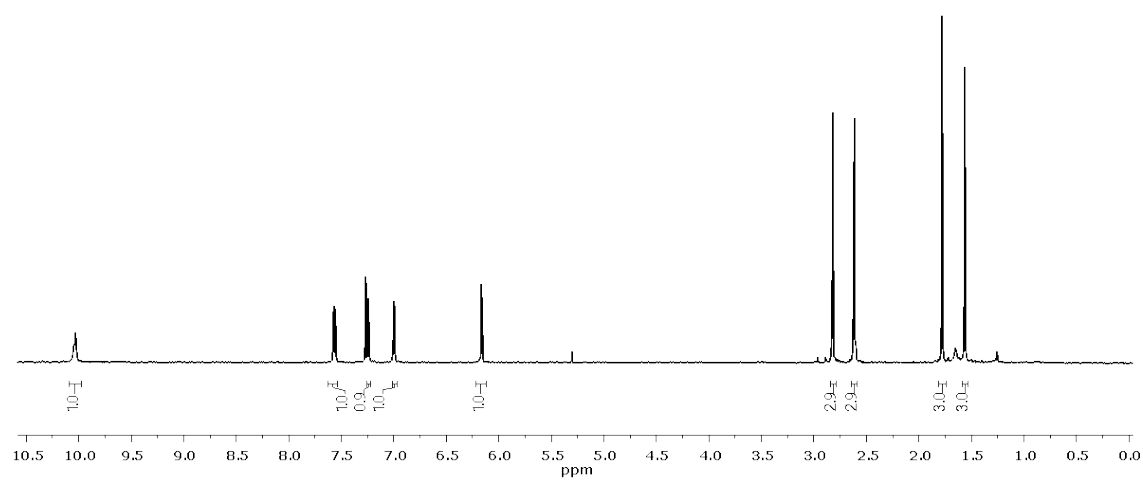


Fig. S7: The ^1H NMR spectrum of **BD2**

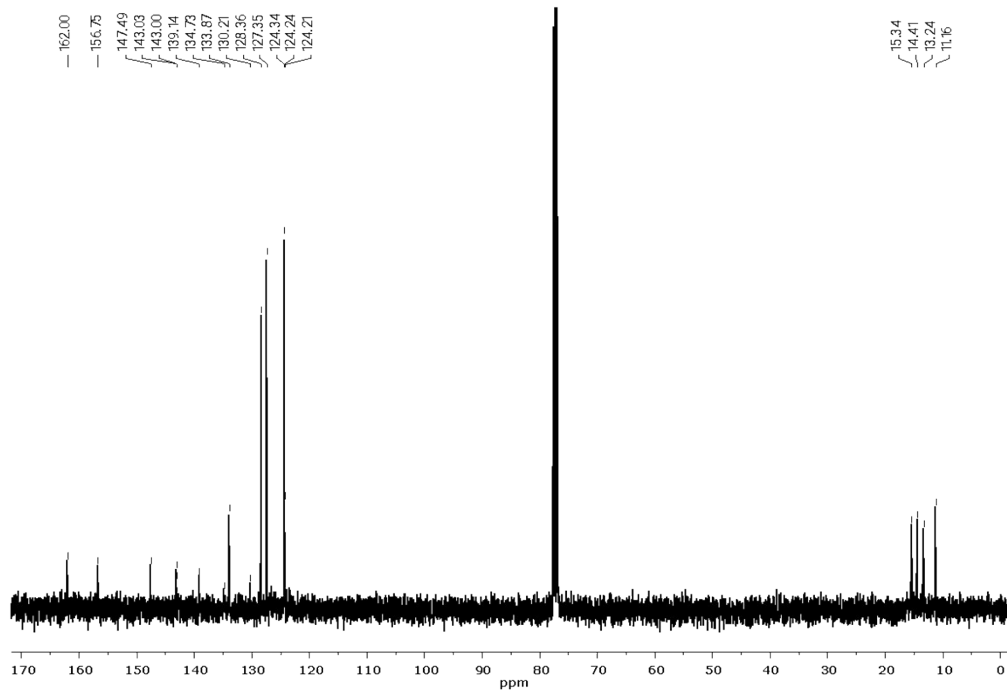


Fig. S8: The ^{13}C NMR spectrum of **BD2**

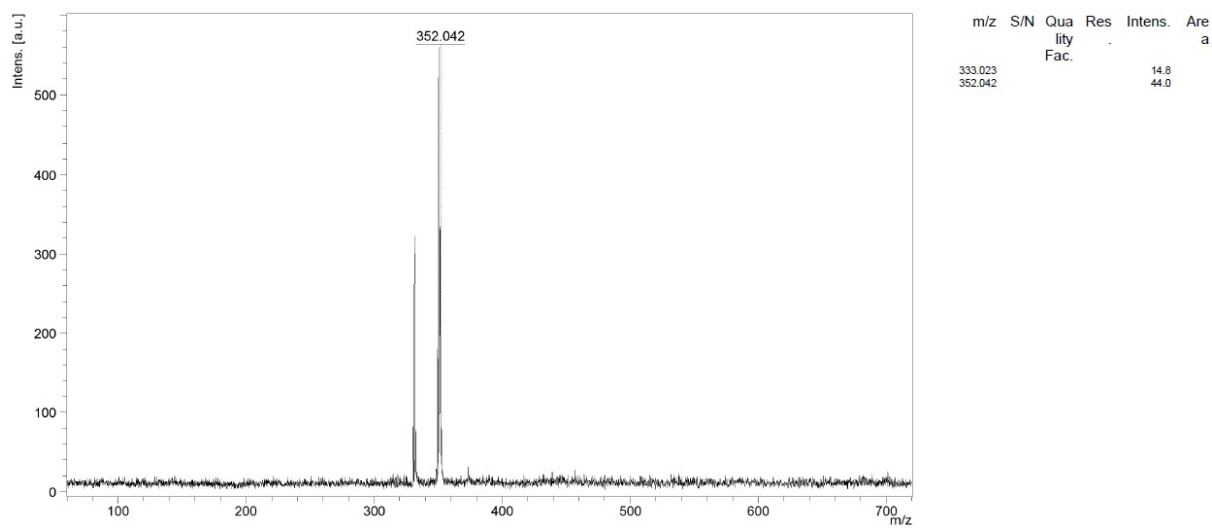


Fig. S9: The MALDI TOF mass spectrum of **BD4**

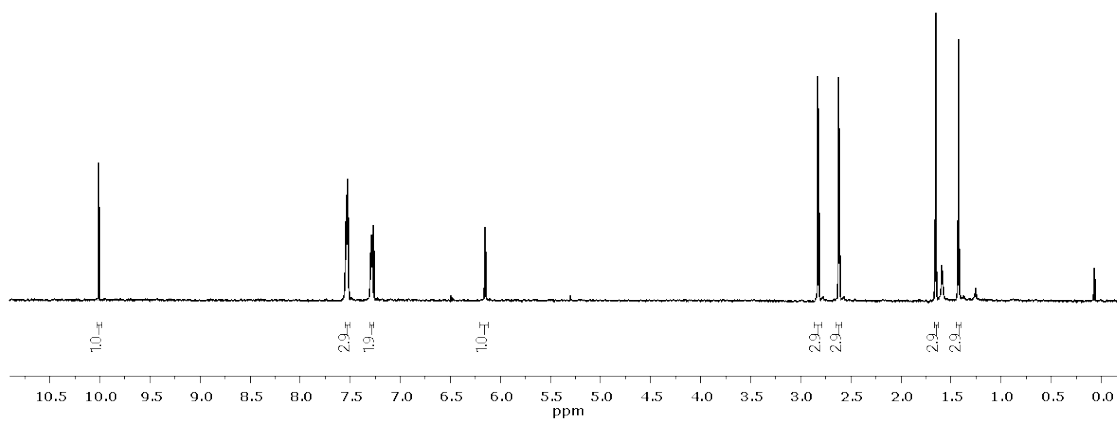
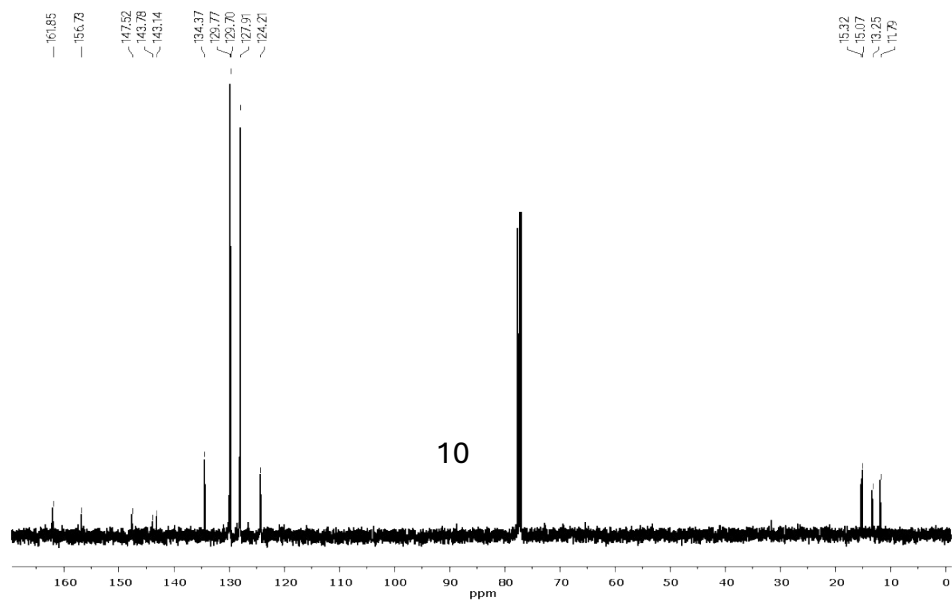


Fig. S10: The ^1H NMR spectrum of **BD4**

Fig. S11: The ^{13}C NMR spectrum of **BD4**



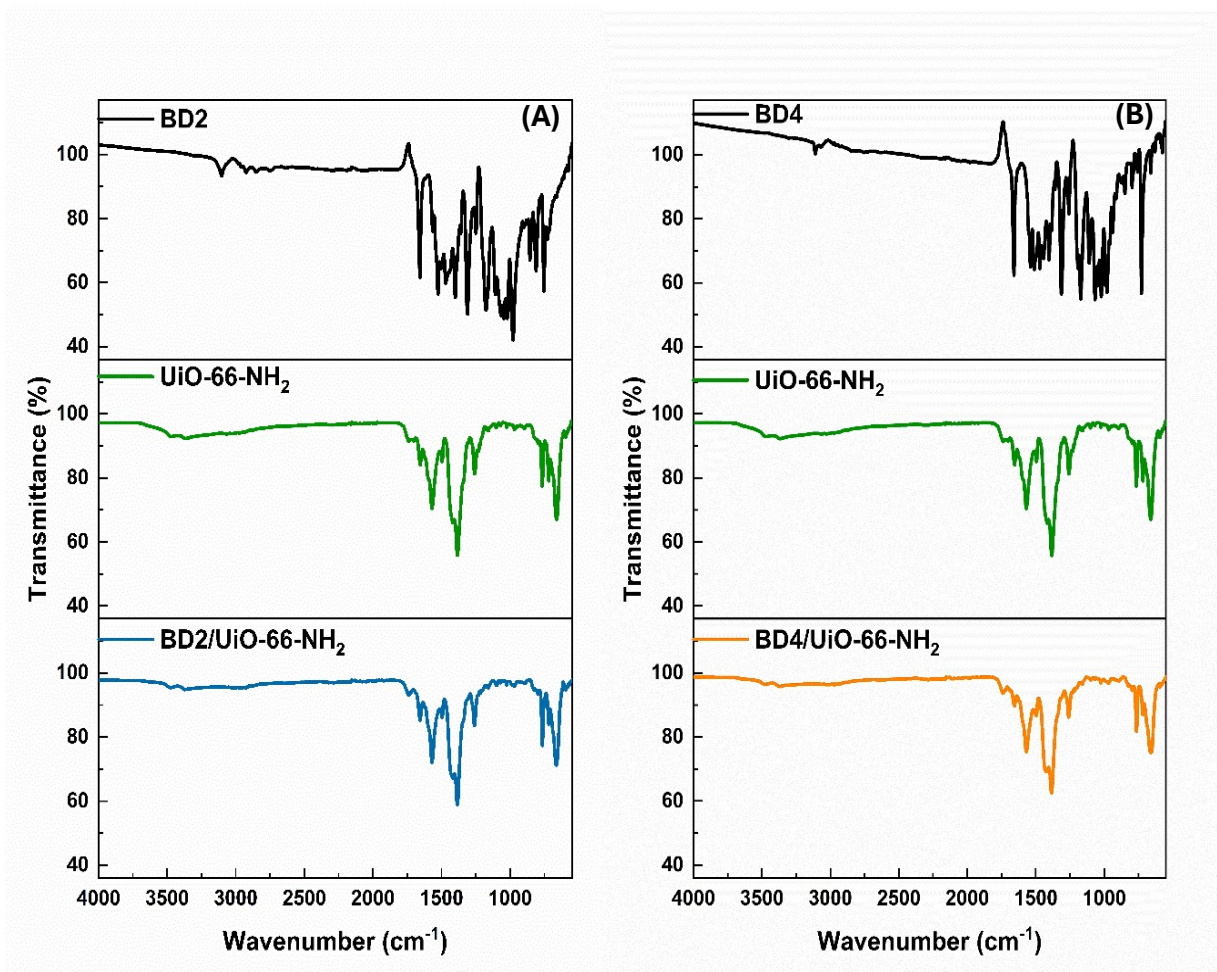


Fig. S12: FT-IR spectrums of (A) BD2/Uio-66-NH₂, (B) BD4/Uio-66-NH₂

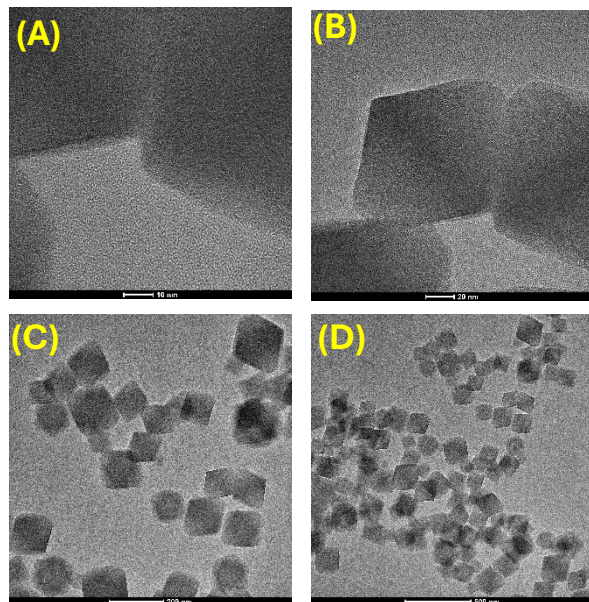


Fig. S13: HRTEM images of UiO-66-NH₂ (A) 10 nm, (B) 20 nm, (C) 200 nm, (D) 500 nm.

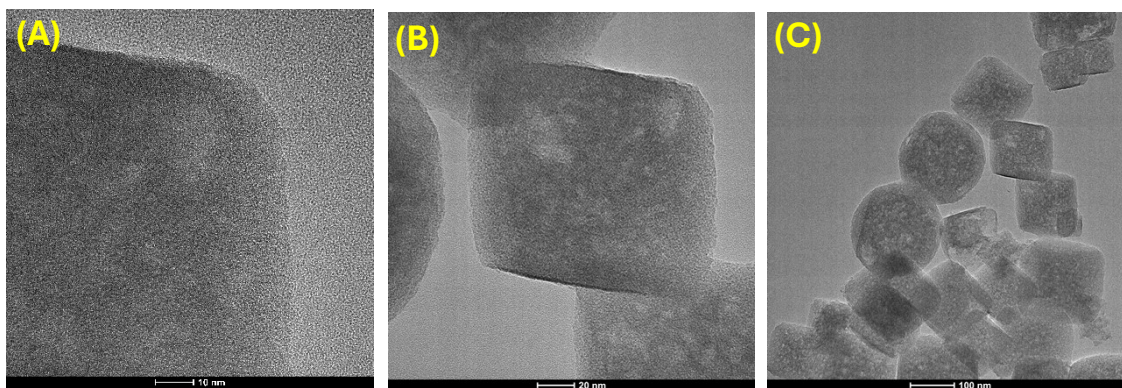


Fig. S14: HRTEM images of BD4/UiO-66-NH₂ (A) 10 nm, (B) 20 nm, (C) 100 nm.

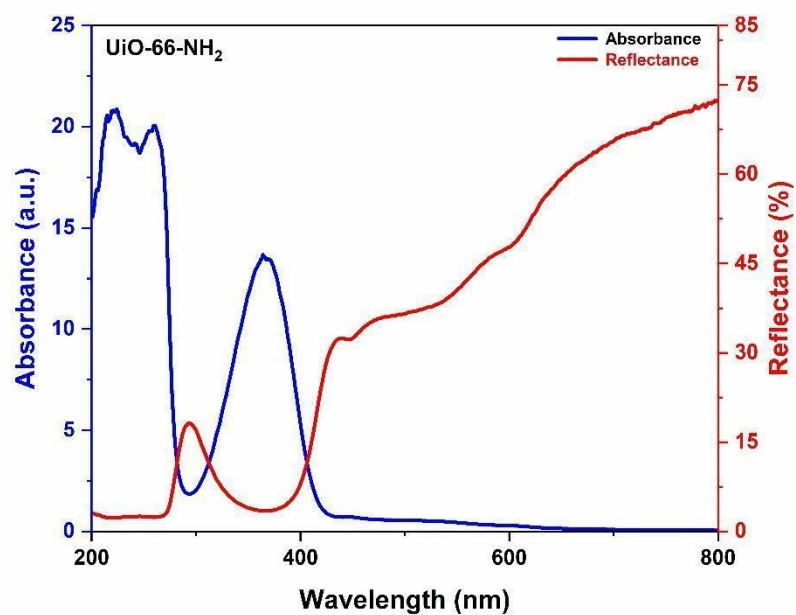


Fig. S15: Absorbance and reflectance spectrums of UiO-66-NH₂.

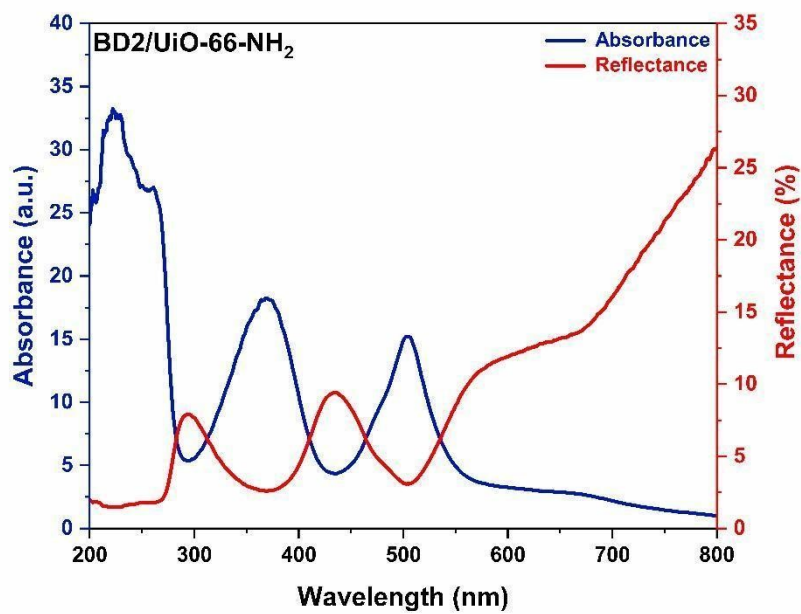


Fig. S16: Absorbance and reflectance spectrums of BD2/UiO-66-NH₂.

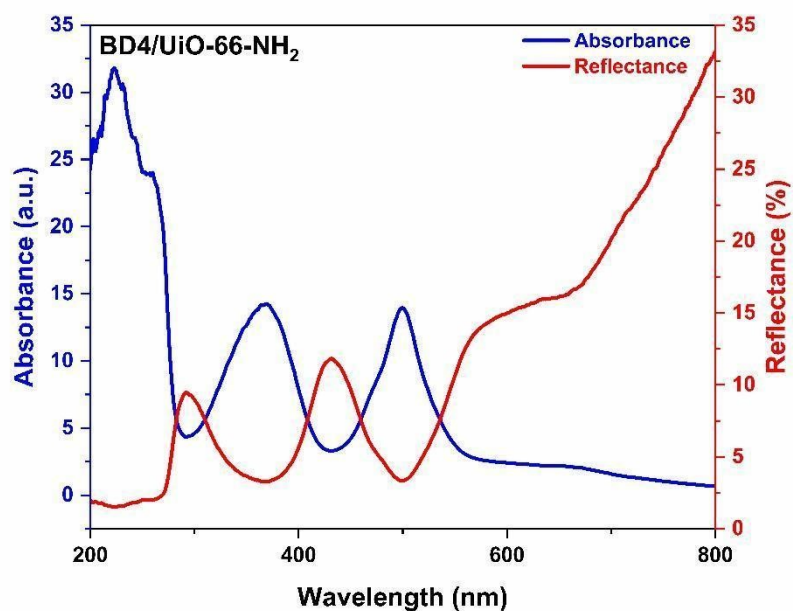


Fig. S17: Absorbance and reflectance spectrums of BD4/UiO-66-NH₂.

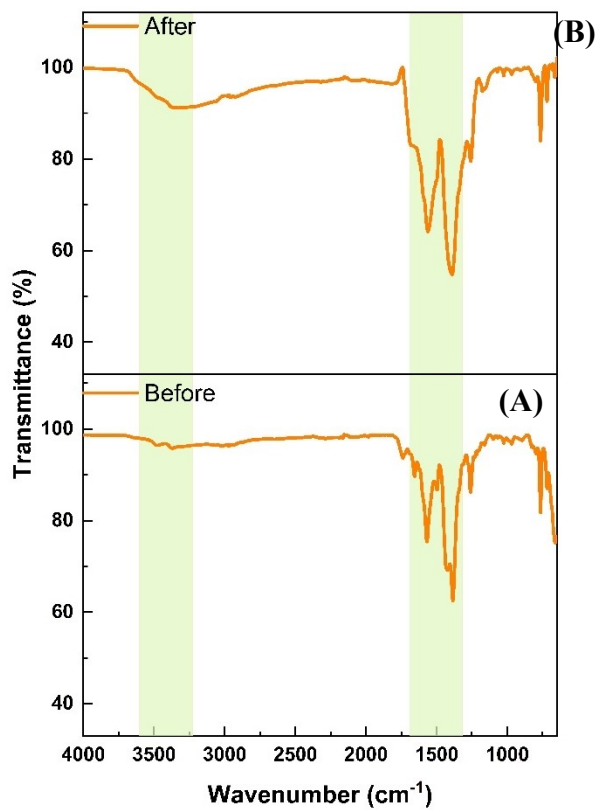


Fig. S18: FTIR spectra of BD4/UiO-66-NH₂ (A) before, (B) after HER

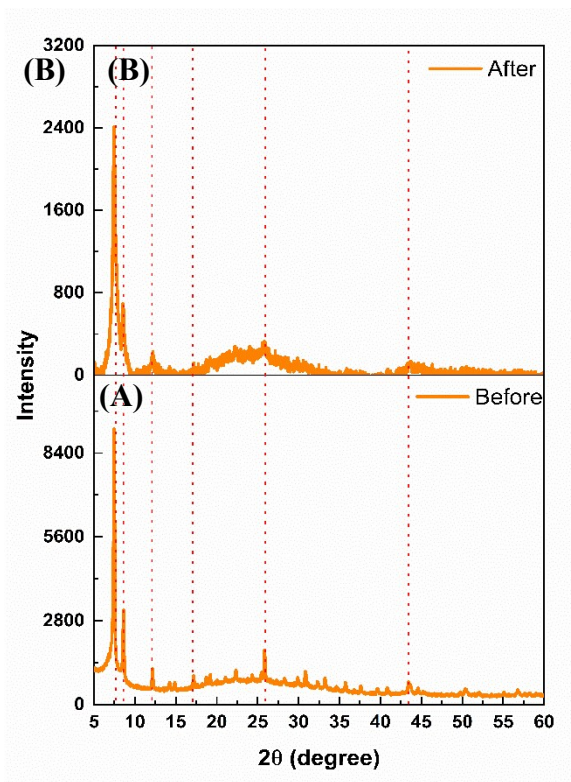


Fig. S19: PXR D pattern of BD4/Uio-66-NH₂ (A) before, (B) after HER

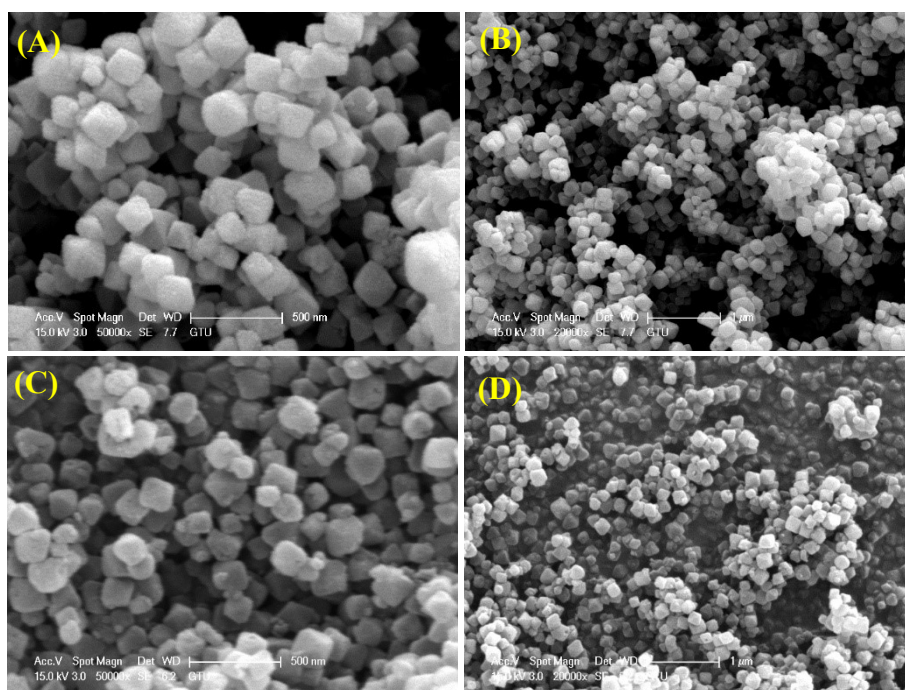


Fig. S20: SEM images of BD4/Uio-66-NH₂ (A, B) before, (C, D) after HER

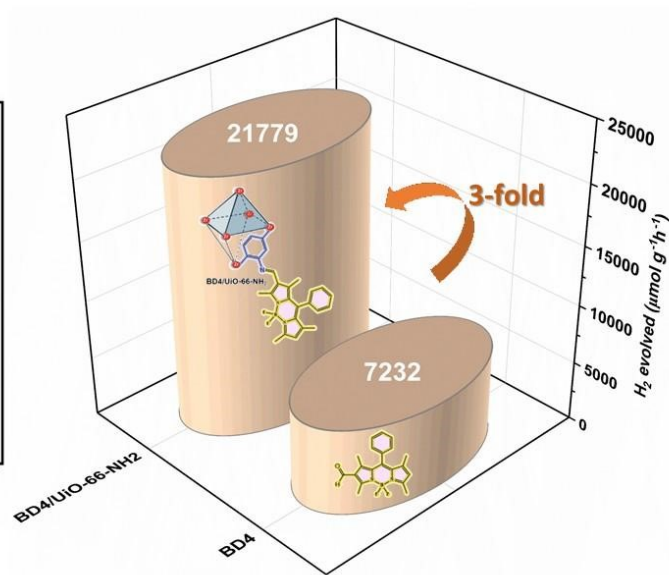
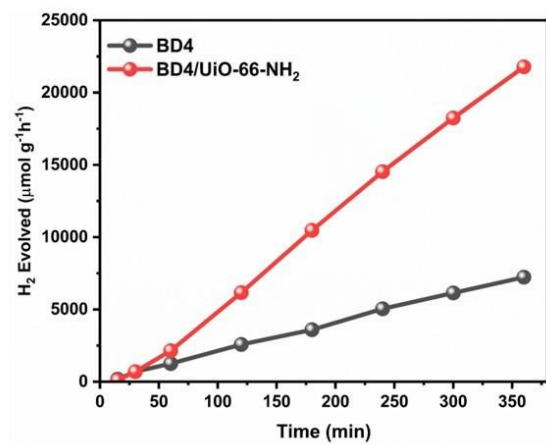


Fig. S21: H₂ Evolution Comparison of BD4 and BD4/Uio-66-NH₂